Three-dimensional X-ray microcomputed tomography of carbonates and biofilm on operated cathode in single chamber microbial fuel cell

Maurizio Santini[a)]
Department of Engineering and Applied Sciences, University of Bergamo, Viale Marconi 5, 24044 Dalmine, Bergamo, Italy

Manfredo Guilizzoni[a)]
Department of Energy, Politecnico di Milano, Via Lambruschini 4, 20156 Milan, Italy

Massimo Lorenzi
School of Engineering and Mathematical Sciences, City University London, Northampton Square, London EC1V 0HB, United Kingdom

Plamen Atanassov
Department of Chemical and Biological Engineering, Center for Micro-Engineered Materials (CMEM), University of New Mexico, Albuquerque, New Mexico 87131

Enrico Marsili
Singapore Centre on Environmental Life Sciences Engineering (SCELSE), Nanyang Technological University, 60 Nanyang Drive, 637551 Singapore, Singapore and School of Biotechnology, Dublin City University, Collins Avenue, Dublin 9, Dublin, Ireland

Stephanie Fest-Santini
Department of Management, Information and Production Engineering, University of Bergamo, Viale Marconi 5, 24044 Dalmine, Bergamo, Italy

Pierangela Cristiani[b)]
Sustainable Development and Energy Sources Department, RSE—Ricerca sul Sistema Energetico S.p.A., Via Rubattino 54, 20100 Milan, Italy

Carlo Santoro[c)]
Singapore Centre on Environmental Life Sciences Engineering (SCELSE), Nanyang Technological University, 60 Nanyang Drive, 637551 Singapore, Singapore

(Received 3 July 2015; accepted 26 August 2015; published 10 September 2015)

Power output limitation is one of the main concerns that need to be addressed for full-scale applications of the microbial fuel cell technology. Fouling and biofilm growth on the cathode of single chamber microbial fuel cells (SCMFC) affects their performance in long-term operation with wastewater. In this study, the authors report the power output and cathode polarization curves of a membraneless SCMFC, fed with raw primary wastewater and sodium acetate for over 6 months. At the end of the experiment, the whole cathode surface is analyzed through X-ray microcomputed tomography (microCT), scanning electron microscopy, and energy-dispersive X-ray spectroscopy (EDX) to characterize the fouling layer and the biofilm. EDX shows the distribution of Ca, Na, K, P, S, and other elements on the two faces of the cathode. Na-carbonates and Ca-carbonates are predominant on the air (outer) side and the water (inner) side, respectively. The three-dimensional reconstruction by X-ray microCT shows biofilm spots unevenly distributed above the Ca-carbonate layer on the inner (water) side of the cathode. These results indicate that carbonates layer, rather than biofilm, might lower the oxygen reduction reaction rate at the cathode during long-term SCMFC operation.

I. INTRODUCTION

Bioelectrochemical systems like microbial fuel cells (MFCs) exploit biological rather than chemical catalysts on both anode and cathode to achieve electrochemical redox reactions that generate current while degrading organic compounds.

Despite extensive research, further insight is needed on electron transfer processes,[1–3] materials performances,[4,5] system design and scaling up,[6] in order to make bioelectrochemical systems competitive with currently used technologies for wastewater treatment. The limitation to the oxygen reduction reaction (ORR) at the cathode and its catalysis,[7] induced by chemical,[8–10] enzymatic,[11,12] or microbial[13,14] mechanisms, are being targeted to increase the MFC power output.

The single chamber microbial fuel cell (SCMFC), without electrolytic membrane between anode and cathode,[15] is likely the most promising design for MFC, due to its simplicity and low cost. Nevertheless, the cathode performance

[a)]M. Santini and M. Guilizzoni contributed equally to this work.
[b)]Electronic mail: pierangela.cristiani@rse-web.it
[c)]Present address: Department of Chemical and Biological Engineering, Center for Micro-Engineered Materials (CMEM), University of New Mexico, Albuquerque, NM 87131; electronic mail: carlo.santoro830@gmail.com

decays with time, due to the long-term exposure to primary wastewater pollutants and dissolved salts that might precipitate when *p*H overcomes the buffer capacity of the catholyte.

In SCMFCs, the direct exposure of the electrodes to the solution enriched with the inorganic/organic substrate and bacteria induces the growth of an electroactive biofilm on both anode and cathode.[16–19] The study of biofilm and biofouling interaction with the electrode materials is therefore crucial for SCMFC understanding and optimization.

Biofilms are microstructured microbiological communities that thrive at the solid/liquid interface. Microorganisms in biofilm produce extracellular polymeric substances that form a cell-encasing matrix whose composition is up to 90% water.[20] Particulates, inorganic precipitates, and corrosion products are also entrapped in the biofilm whose composition depends of the environment and the substrate.[20–22] The characterization of the physicochemical and structural properties of biofilms is crucial for bioelectrochemical systems optimization. Previously reported techniques for biofilm structural characterization include optical sectioning,[23] FTIR analysis,[24] and other microscopy methods.[25–29]

While commercial sensors and microsensors can be used to characterize the chemical makeup of biofilm, including thick environmental biofilms, there is no simple technique available to determine the morphological features of a thick biofilm (i.e., having a thickness of a few millimeters). Certain microsensors can be used to determine porosity and local mass transfer properties, but the experiments are time-consuming.[26,27] Simple microsensors have also been used for measuring *p*H, redox potential, oxygen content, and OH^- concentration, with good accuracy.[30–33]

In early biofilm studies, thick biofilms were cut in thin sections and imaged through fluorescence microscopy and the 3D images were then reconstructed by common image analysis algorithms. Modern multiphotons confocal laser scanning microscopies (CLSM) are ideal for nondestructive imaging of most biofilms and to identify bacteria in the biofilms settling on the anode or cathode surface of bioelectrochemical systems. However, the resolution of the CLSM images decreases when the biofilm is thicker than 0.3–0.5 mm, because of photon scattering. Furthermore, microscopy analysis requires staining protocols or the expression of green fluorescent protein in the microorganisms to improve the visualization of details. Other techniques, such as scanning electron microscopy (SEM), require harsher drying pretreatment that often lead to the formation of structural artifacts.[34,35]

Three-dimensional X-ray microcomputed tomography technique (microCT) is a nondestructive method that enables imaging and 3D reconstruction of complex microbiological structures, regardless of their thickness. Therefore, it is a suitable method for the characterization of the thick biofilms that grow in SCMFC after long-term operation with wastewater.

The electrochemical analysis of cathode performance and the overall voltage of a SCMFC running for over 6 months are presented in this work. Furthermore, the SCMFC cathode was imaged through microCT and other imaging methods at the end of the 6 months experiment, to characterize the biofouling layer and the biofilm. Results show that the thick fouling layer on the SCMFC cathode limit the ORR, thus the overall power output.

II. MATERIALS AND METHODS

A. SCMFC assembly, working conditions, and electrochemical measurements

The membrane-less SCMFC [Fig. 1(a)] was assembled as previously described.[17] Briefly, a borosilicate glass (Pyrex®) bottle of 125 ml was equipped with a large Pyrex flange on one side, to accommodate the open-air cathode. The bottle was sealed airtight with plastic screw cap to prevent air leakage into the anolyte. Raw primary wastewater from Milano-Nosedo treatment plant (Milan, Italy) was inoculated in the anode compartment. The wastewater has *p*H equal to 7.9 and COD $< 500\,\mathrm{mg\,l^{-1}}$ (Chemical Oxygen Demand). Particularly, the treatment plant monitored the wastewater finding the following concentration of some chemicals of interest: 0.1 $\mathrm{mgN\text{-}NH_4^+\,l^{-1}}$, 5.5 $\mathrm{mgN\text{-}NO_3^{-1}\,l^{-1}}$, 6.4 $\mathrm{mgN_{tot}\,l^{-1}}$, 0.8 $\mathrm{mgP\,l^{-1}}$, 75 $\mathrm{mgCl^-\,l^{-1}}$, and 60 $\mathrm{mgSO_4^{2-}\,l^{-1}}$. Moreover, also turbidity (1 NTU) and conductivity ($725\,\mu\mathrm{S\,cm^{-1}}$) have been measured. After

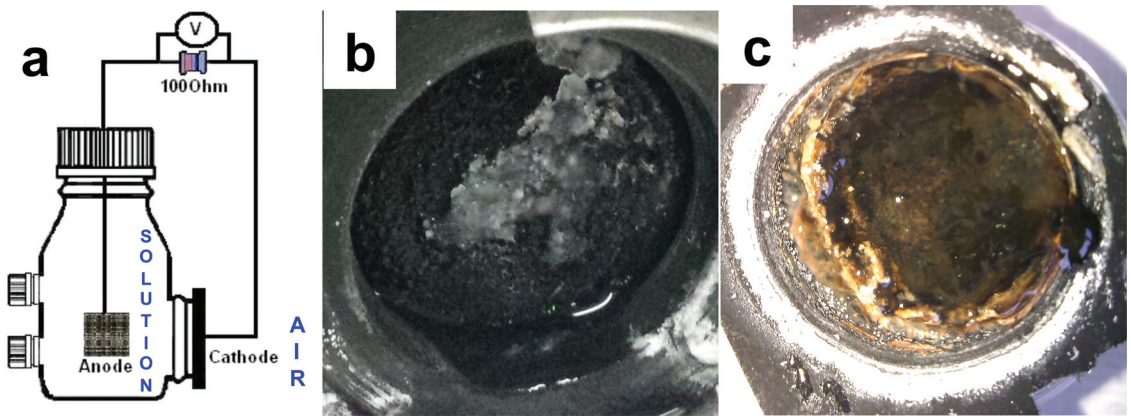

FIG. 1. (a) Schematic of the batch MFC used in this study; (b) outer side of the air cathode; and (c) inner side of the air cathode after 6 months of operation.

inoculum, 10 mM sodium acetate (Sigma-Aldrich, Italy) was added periodically to maintain nonlimiting concentration of electron donor in a batch operation. The SCMFCs worked at room temperature that was roughly constant and equal to 21–23 °C. The cathode was built similarly to a previously reported protocol.[36] A 30×30 mm carbon cloth (SAATI C1) was coated with a microporous layer (MPL) (TIMCAL ENSACO 350G + Nafion® ink) on the inner surface (i.e., facing the anodic compartment) and a gas diffusion layer (GDL) (TIMCAL ENSACO 350G + 80% Polytetrafluoroethylene (PTFE) ink) on the external surface (i.e., facing air).[37] The external gas diffusion layer guarantees mechanical stability in long term operation.[37]

The geometrical surface area exposed to the solution was a circle having a diameter of 20 mm. The anode was made of 20×50 mm carbon cloth (SAATI C1, SAATI Legnano, Italy) without modification. Anode and cathode were connected to an external resistance of 100 Ω, and the voltage was recorded every hour during the 6 months experiment. At day 5, 14, 30, 50, 90, and 145, the cell was disconnected and the cathode polarization curve was taken. The SCMFC was left in open circuit potential (OCP) for at least 1 h, and then, the linear sweep voltammetry was performed from OCP to −0.4 V versus SHE at a scan rate of 0.167 mV s^{-1}.[17]

B. Cathode imaging

After 6 months operation, the cathode was removed from the SCMFC, photographed and then cut in small pieces (10×15 mm) for SEM and 3D X-ray microCT. After air drying for 3 days, part of the samples was coated with graphite to increase surface conductivity and then analyzed with SEM–energy-dispersive X-ray (EDX) (Mira II Tescan).

X-ray microCT of the cathode was carried out modifying a previously published protocol.[38,39] The wet cathode sample was inserted into a sealed polycarbonate tube (transparent to X-ray) to avoid drying of the sample during the time needed for the microCT analysis. In turn, this set up avoids dehydration of the biofilm sample and degradation of the biofilm structure, which is a serious problem in SEM imaging. A tungsten-anode X-ray microfocus source was used to radiate the specimen. The transmitted and attenuated X-ray intensity was projected onto a high-resolution X-ray detector system. The sample was slowly rotated along one reference axis on a high-precision rotation stage, and several hundred projections were collected as described in previous works.[40,41] The 3D volume of the sample was reconstructed from such projections using tomographic reconstruction algorithm based on the Filtered Back Projection.[42] From the reconstructed volume, intensity isosurfaces representing the 3D surface of the sample could be also extracted. A 10×15 mm sample of the cathode was analyzed by microCT immediately after disassembling the cell. From the total reconstructed volume, a subvolume (5×5 mm) was also extracted for the quantitative measurement described in Sec. III D.

III. RESULTS

A. Electrochemical performance and cathode visual inspection

After six months, the operated SCMFC was disassembled and the cathode was imaged through several methods. A picture of the air-side surface of the cathode is reported in Fig. 1(b) and the water-side one in Fig. 1(c).

The overall SCMFC voltage and power with time are reported in Fig. 2(a). The power output increased in the first 3 weeks, and then decreased almost linearly over time. The initial increase of the power output was mainly due to the anode, which was slowly colonized by electroactive biofilm that degrades organics and release electrons on the conductive carbonaceous electrode.[36] The maximum power output of 55 μW was produced after 20–22 days. The cathode polarization curve [Fig. 2(b)] shows that electroactivity increased from day 5 to day 14 and steadily decreased with time.

The visual inspection of the SCMFC cathode revealed a thick biofilm on the inner side (i.e., facing the anodic compartment) covering a white precipitate [Fig. 1(c)]. The biofilm coverage was not homogeneous and the electrode was partially black, likely because of sulphide residuals.[17] A white ring of soluble (sodium carbonate) deposit was also visible, external to the o-ring sealing the SCMFC. The cathode side facing air showed a thinner white deposit with no

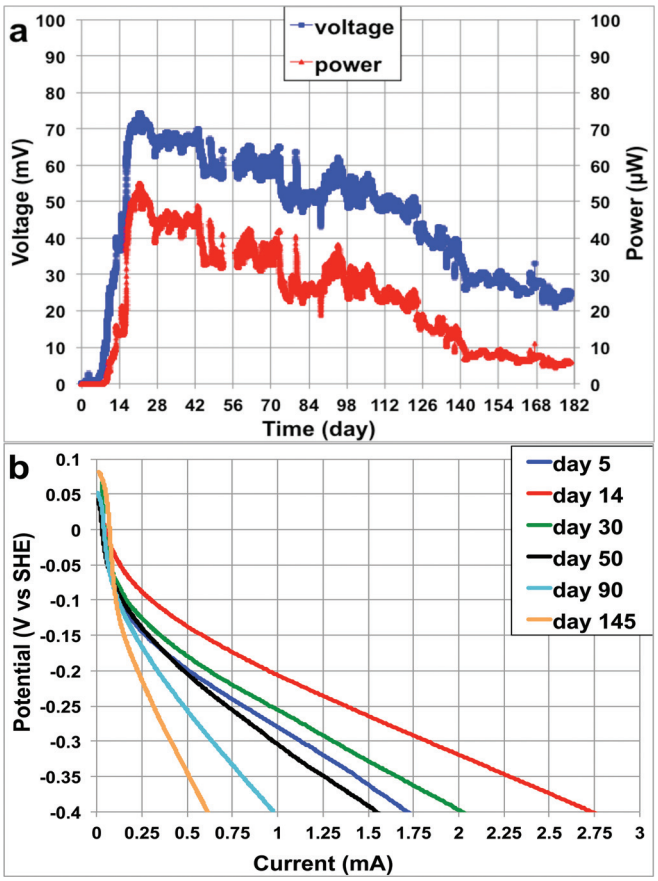

FIG. 2. Voltage recorded over 100 Ω external resistor (blue) and power (red) (a), polarization curves of cathodes over 145 days experiments (b).

biofilm growth, made of sodium carbonates like that one external to the o-ring, on the other side [Fig. 1(c)].

A white carbonate deposit on the cathode has been already observed and chemically analyzed, in previous long-term experiments with SCMFCs.[17,36,43–48] The white Na-carbonate was probably due to leakage of catholyte. The Ca-carbonate, less soluble than Na-carbonate, precipitated on the cathode inside the solution.

B. SEM imaging and EDX analyses

The SEM–EDX images of the cathode are reported in Fig. 3. The outer side of the cathode [Fig. 3(c)] shows a smooth surface due to the partial melting of the PTFE coating, with salt crystals covering homogeneously the cathode surface [Fig. 3(c)]. The EDX analysis shows high amount of Na, indicating precipitation of Na-carbonates [Fig. 3(c)]. The visual appearance of the inner side of the cathode differs

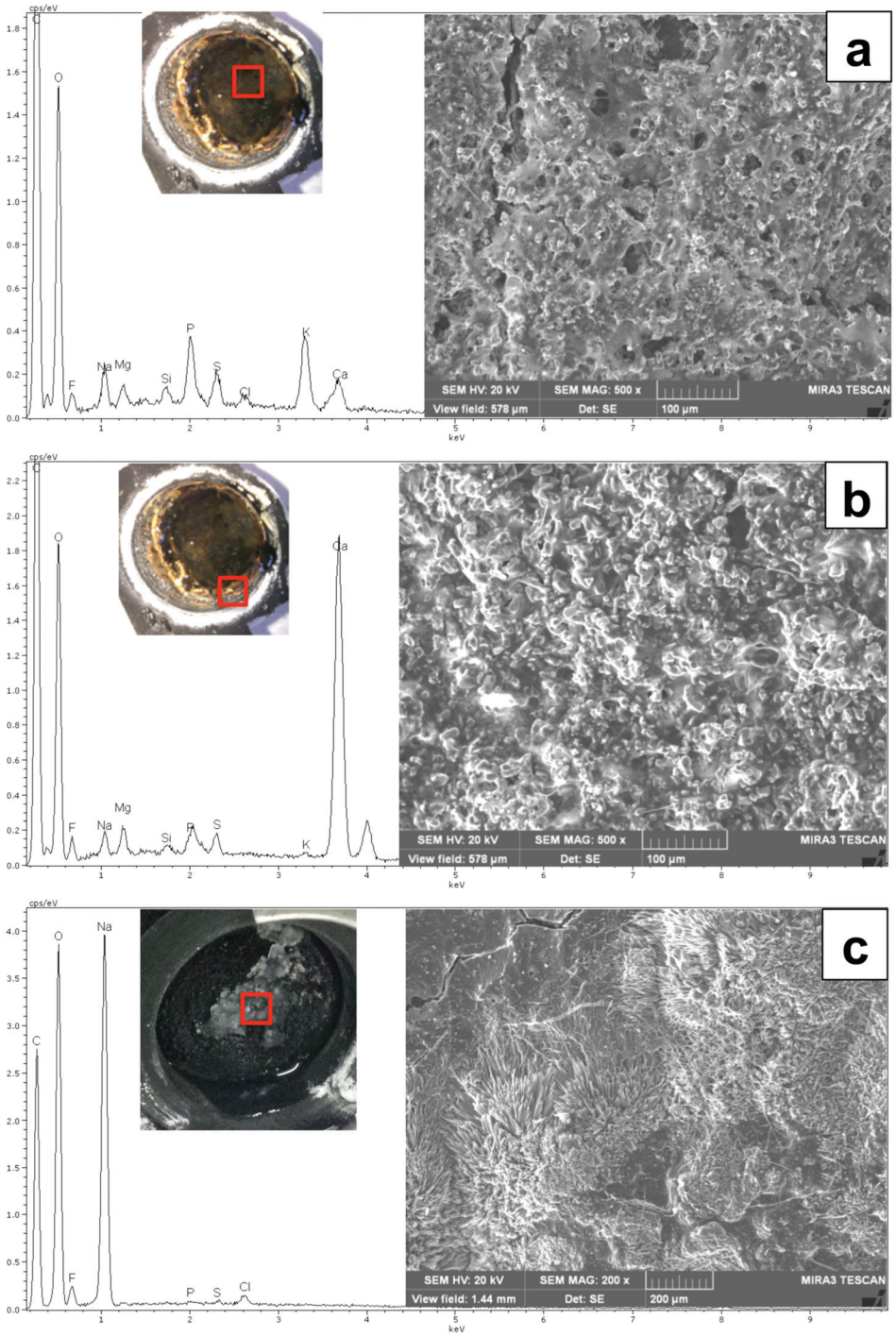

FIG. 3. SEM micrographs and EDX analysis of the scaling on the cathode: inner face [(a) and (b)] and outer face (c). Red squares identified the region on the sample where the micrographs have been selected.

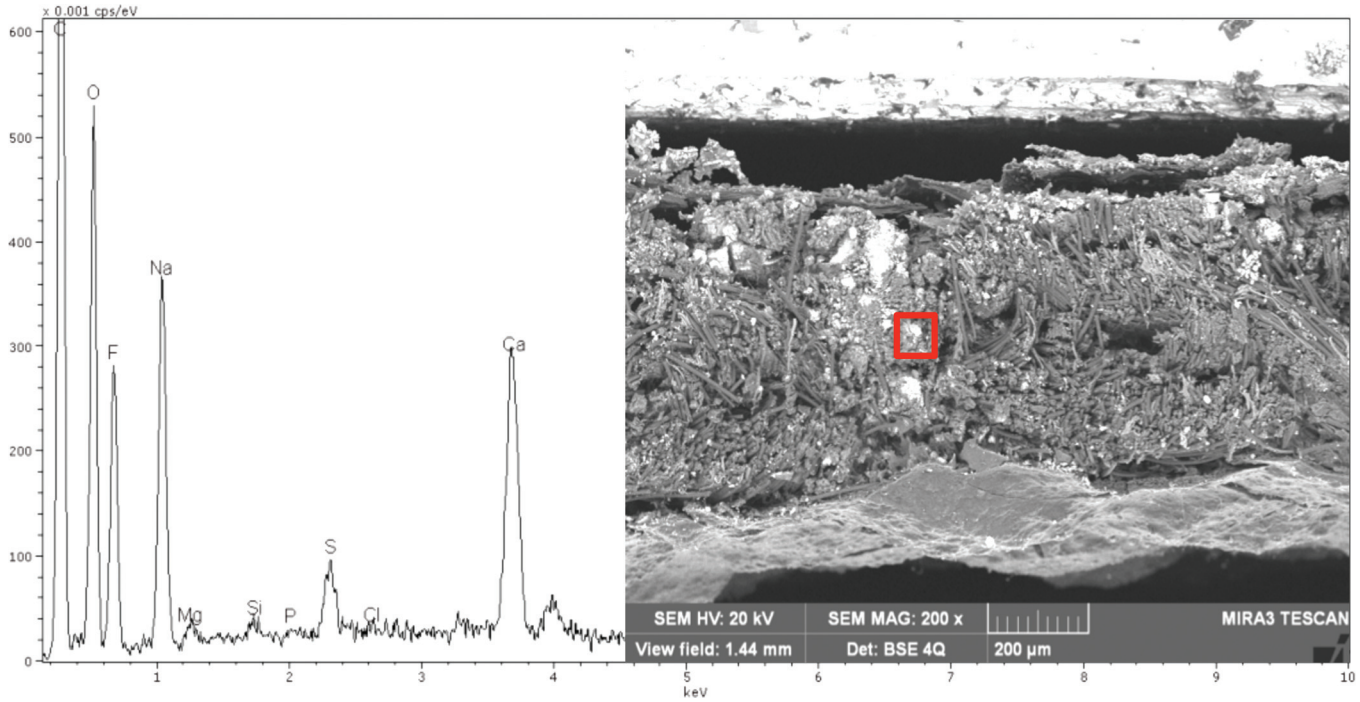

FIG. 4. SEM micrographs of the cross-section of the cathode and EDX diffractogram. Red squared identifies the region on the sample where the micrographs have been selected.

between the center and the periphery of the electrode. In the center, Na and Ca peaks were observed mixed with other elements (S, P, and K) typical of biofilms. In the periphery, where biofilm is less significant, Ca carbonates were predominant. P and S peaks were detected only in the inner side of the cathode. Outside the cathode [Fig. 3(c)] the peak of Na underlined the different nature of the deposit.

The SEM of the cross section (Fig. 4) evidences the presence of carbonates scaling the wires of carbon cloth texture while the EDX graph shows the Na- and Ca-carbonates precipitate. The salt crystals extend also in the fibers of the electrode material. These results are consistent with previous EDX analyses, where Ca^+ and K^+ precipitates were observed on the SCMFC cathodes together with their corresponding carbonates.[17,43]

The uniformity and homogeneity of the Ca-carbonate layer is not evident from the micrographs in Fig. 3. On the contrary, Fig. 3 shows that a cracked and whitish deposits of carbonate alternates to biofilm and the other cathode components.

C. X-ray microCT imaging

X-ray microCT images of the SCMFC cathode are presented in Figs. 5–8. The video scan of the section of the cathode sample is in Fig. 8. The biofilm/fouling grown on the anolyte side [top part, Fig. 5(a)] of the cathode had higher roughness than that grown on the air side [Fig. 5(b)]. This is consistent with the SEM results. Fractures and defects in the PTFE layer of the air side of the cathode were likely due to the rapid cooling after the heating treatment.

X-ray microCT images cannot be compared directly with SEM, because of the pretreatment of SEM samples and the different resolution, which is 5.12 μm voxel size for microCT. The lower resolution of microCT is compensated

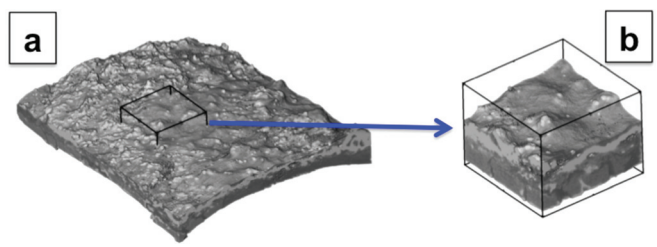

FIG. 5. Grayscale rendering of the cathode reconstructed by X-ray microCT evidencing the morphology of the internal face of the cathode and two side cross-sections. Full reconstructed volume (a) and an extracted subvolume to better evidence structure details (b). The top surface represents the cathode side facing the solution.

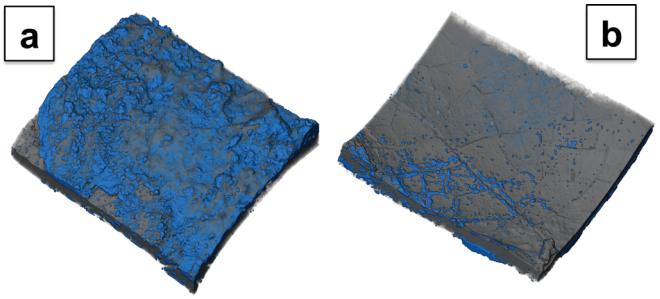

FIG. 6. X-rays microCT images of the internal (a) and external (b) face of the investigated cathode, underlined with the blue color is the presence of carbonate precipitation.

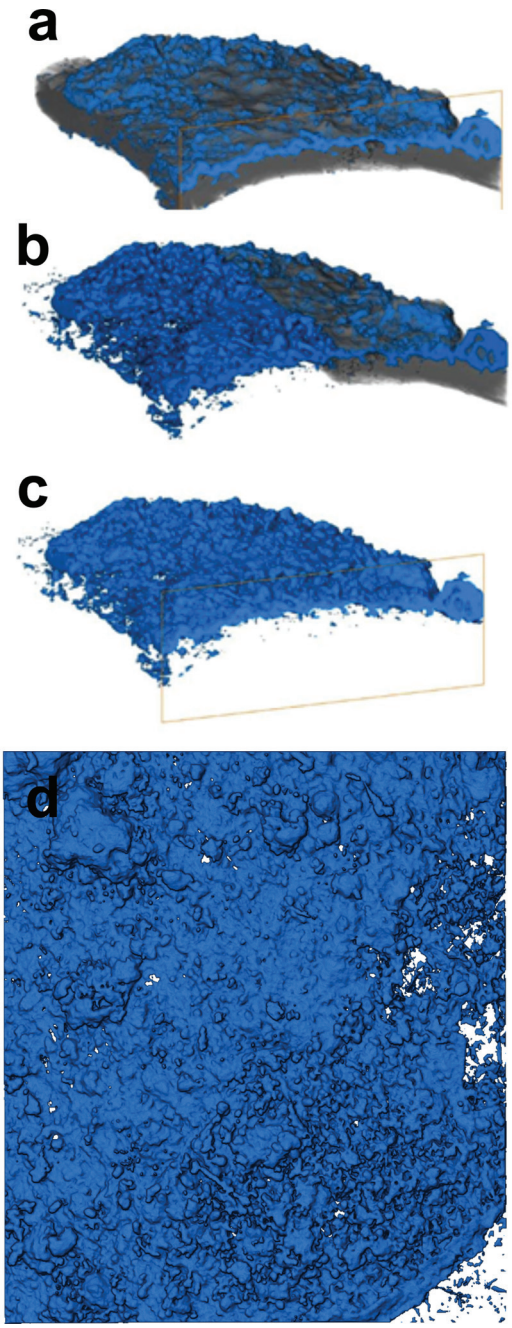

FIG. 7. Segmentation of the total reconstructed microCT volume to extract the full cathode sample (a), the sample after partial (b) and total [(c) and (d)] removal of the cathode material and biofilm, to evidence the carbonate precipitation layer.

by the 3D imaging of the sample that is not possible through SEM.

D. X-ray microCT postprocessing

Three-dimensional reconstruction of volumes from microCT images are represented in grayscale using the FBP algorithm, where lighter color indicates lower X-ray attenuation (i.e., lower atomic density); hence, this technique allows distinguishing biofilm from inorganic fouling based on the average atomic number Z of each voxel (3D pixel).

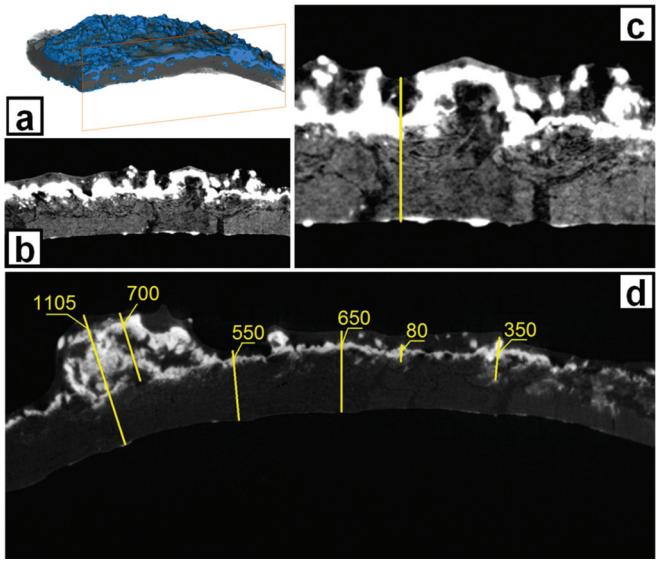

FIG. 8. Orthogonal cross-section of the cathode sample extracted from the reconstructed microCT volume and postprocessed to extract estimated thickness information (dimensions in micrometer); in (c) the line is equal to 650 μm (enhanced online) [URL: http://dx.doi.org/10.1116/1.4930239.1].

In Figs. 6–8, the region of highest X-ray attenuation is rendered in blue and corresponds to the carbonate precipitation through the biofilm by comparison with the SEM images. Carbonate precipitation can be clearly observed on the internal face [Fig. 6(a)] and in a few areas of the external face [Fig. 6(b)] of the cathode, where the GDL layer was cracked, or completely missing. The purpose of the external PTFE/CB (Carbon Black) layer is mainly to prevent water leakage from the inside of the SCMFC to the outside, while allowing oxygen penetration to the catalytic side where oxygen reduction reaction occurs. Figure 6(b) shows carbonate precipitation along the fractures of the PTFE/CB external layer, underlining surface defects that might have been worsened by the penetration of precipitants into the external surface. Benzinger *et al.*[49] showed that a large pressure differential, several meters of water column are necessary to allow liquid permeation through the wet-proofed carbonaceous electrode commonly used in a hydrogen PEM fuel cell. These results are consistent with previously reported findings,[47] showing through SEM images that the carbonates deposits forming on the electrode over 3 months causes the degradation of the electrode texture and structure.[47]

The microCT reconstructed image of the cathode [Fig. 7(a)] was processed to separate the biofilm from the carbonate precipitate and the electrode material. The cathode materials and the biofilm were partially [Fig. 7(b)] and completely [Fig. 7(c)] removed, showing only the thick layer of carbonate precipitation [Fig. 7(d)] that appears compact and extend along the entire inner cathodic surface.

X-ray microCT reconstructions also allow extracting quantitative information. A 5×5 mm subvolume of the cathode was selected to this purpose. Given the low curvature of the subvolume, the total surface area was $25 \times 2 = 50\,\text{mm}^2$

(considering both bottom and top surfaces). Within this subvolume, the total carbonate volume was 3.8 mm^3, corresponding to about 0.15 mm^3/mm^2 of surface. This value is consistent with the X-ray microCT measures along the cross-sections of the cathode, where the total surface area of the carbonate precipitation was 127.9 mm^2, to be compared with the total 50 mm^2 surface area of the analyzed subvolume. This value too seems credible given the very complex and indented external surface of the carbonate layer.

Selected cross-sections of the reconstructed volume show that the precipitate layer on the inner cathodic surface was compact, approximately uniform and in direct contact with the cathode surface. However, the biofilm grew above the precipitate layer and it was not uniform (Fig. 8).

IV. DISCUSSION

A. Mechanisms of carbonate precipitation at the cathode

In a typical membrane-less SCMFC, the cathode faces the anolyte on the inner side and the atmosphere on the outer side. The modification of cathode surface with GDL allows oxygen penetration through the porous carbon material to the catalytic sites, where ORR occurs, minimizing water leakage. On the other hand, application of MPL enhances bacteria attachment. The hydrophilic/hydrophobic gradient that establishes in the MPL and GDL-coated cathode from the internal to the external side includes the three phases catalyst sites (solid–liquid–gas) improving the ORR rate. The three phases interface is fundamental for an efficient ORR guaranteeing electron transfer (solid phase), proton transfer (liquid phase) and oxygen permeation (gas phase).[50] Oxygen diffusion on the inner side of the cathode creates favorable conditions for the growth of a thick mixed species biofilm on the cathode.[13–17] The performance of the SCMFC changes during long-term operation as biofilm and inorganic fouling settled on the cathode.[17,43–45]

Previous studies conducted using phosphate buffer and acetate explained the decreasing in cathode oxygen transfer after 1 year operation with biofilm formation and organic matter accumulation that clogged the cathode pores.[44] The expected performance decrease was much slower in that case, compared to real wastewater that has lower buffering power and contains multiple other cations (e.g., Ca). Those previous studies[44,45] were made in model artificial wastewater and did not include the role of carbonate and might have underestimated its role in decreasing MFC performance. Moreover, they suggested that the development of a thick biofilm impaired the MFC performance probably due to proton mass-transfer limitation at the inner side of the cathode.[44]

In contrast, other studies suggest that the microaerophilic and anaerobic microorganisms in the biofilm grown on the inner side of the cathode enhance its catalytic activity, possibly through NO_3^- or SO_4^{2-} reduction, after few weeks of growth, hence the MFC cathode is termed biocathode. It was early hypothesized that mainly the salt precipitation at cathode, and not a thick biofilm, causes the degradation of the MFC performances.[16,17]

Finally, a recent study demonstrated that an aggressive cathode cleaning procedures using HCl, after long time operation, resulted in performance recovery of 85%. Those data[45] underlined the positive effect of removal of inorganic fouling from the cathode structure rather than organic fouling.

The microCT images of the cathode reported in Figs. 5–8 suggest that biofilm does not play a relevant role in mass transport limitation, as they show that biofilm is patchy, not uniformly distributed and not uniformly thick. Furthermore, the biofilm it is not directly in contact with the inner cathode surface, because of the thick calcium carbonate layer deposited on the surface. The biofilm is much thinner than the carbonate layer, so it is likely that biofilm does not limit ion transport to the cathode.

The precipitation of alkaline salts on the cathode in a membrane-less SCMFC is related to the ORR process and depends on (1) the catalyst used on the cathode;[51] (2) the electrolyte *p*H;[52] and (3) organic substrates used.[53]

The absence of Pt catalyst in the cathode led to a two-electrons ORR, through H_2O_2 reduction to H_2O at low *p*H or to OH^- at high *p*H. At circumneutral *p*H, both reactions might occur with the simultaneous production of H_2O and OH^-. The presence of the OH^- and increase in *p*H close to the cathode has been previously documented[31,52] and this facilitates the carbonate precipitation. In fact, it has been showed previously that *p*H might increase locally up to 12 close to the cathode surface,[31,54] although the oxidation of sodium acetate used as organic substrate might partially balance the consequent alkalinization on the cathode.[53]

The uniform carbonate layer might play an important role in the decaying of the overall SCMFC performance. It might be assumed that the thick and compact carbonate layer causes ions mass transport limitations, eventually impeding the contact between the solution and the active, conductive catalytic sites of the cathode.

B. Use of X-ray microCT to explain the cathodic SCMFC mechanism

Only SEM/EDX characterization of MFC cathodes have been previously reported,[17,36,43–48] showing that calcium and sodium carbonate accumulate on the MFC cathode. However, X-ray 3D microCT is preferable over SEM because it provides the 3D distribution of the precipitates. SEM, on the other hand, requires sample pretreatment, which can damage the inorganic fouling layer. Furthermore, SEM can be used only for surface analysis, while 3D tomography is suitable for thick, compact samples. X-ray microCT images reported provide relevant insight on the cathode structure after long-term SCMFC operation with wastewater. The carbonate deposition layer on the inner side of the cathode is continuous and thicker than 0.1 mm, and it fills also the pores and cracks of the cathode material on both the inner and the outer cathodic surface. It is likely that the

cathode performances decrease drastically due to this layer of carbonate species, impenetrable for protons, and not because of the biofilm, whose thickness seems too low to inhibit the cathode performances. These findings suggest that carbonate precipitation on the cathode should be minimized and the stability of the GDL on the cathode should be improved, to maintain stable SCMFC performance during long-term operation.

V. COMPARISONS WITH OTHERS IMAGING TECHNIQUES

Electrode imaging in bioelectrochemical system requires often a combination of methods to characterize the electrode surface, the biofilm morphology on the electrode, and the inorganic fouling. Digital imaging and video show the overall electrode *in situ*, but do not provide sufficient resolution to characterize the biofilm and the fine details of electrode surface. SEM offers a submicrometer resolution of the fouling surface or electrode section, but the drying pretreatment increases chances of artifacts and morphological distortions. While glutaraldehyde fixation and ethanol washing steps[28,35] can reduce the extent of artifacts, they cannot be avoided.[28,35] The recently developed environmental SEM allows the imaging of the biofilm also in wet conditions,[55] thus avoiding bacterial fixation artifacts and biofilm morphology distortions. However, this technique is quite complex and requires a dedicated instrument with a special detector. Coupling of SEM with EDX allows understanding of the electrode surface chemistry, particularly the detection of monovalent and divalent cations (Na^+, K^+, Ca^{2+}, and Mg^{2+}) mainly associated with their carbonate species. However, SEM–EDX is a surface characterization method, as electrons cannot penetrate beyond the conductive surface. CLSM imaging is arguably the most common nondestructive method in use for imaging biofilm with minimal pretreatment[28,35] and has been used to image cathodes from bioelectrochemical systems only in double chambers MFC systems.[28,35] Photons can penetrate 300–500 μm of biofilms with submicrometer accuracy, therefore providing excellent understanding of microorganism's location and interaction in mixed microbial biofilm consortia.[28,35] However, optical access to biofilm is required for CLSM analysis and only small samples (i.e., 200×200 μm) can be imaged in a reasonable time. Furthermore, CLSM cannot be used to image inorganic fouling layers such as the carbonate deposits commonly observed in MFC cathodes, as they are impenetrable to photons.

X-ray microCT imaging allows a volumetric investigation of MFC electrode without the abovementioned limitations, and it can be used to analyze both the surface and the deep layers of biofilm and inorganic fouling in their native state, without pretreatment. Postprocessing allows 3D reconstruction, segmentation of the volume, and image analysis to unveil details such as surface defects, density of the fouling layers, and the interface between biological and inorganic fouling. Following calibration with standard volume samples, microCT allows quantitative measure of distance and volumes (at micrometer resolution) within the MFC cathode or other specimen from bioelectrochemical systems. Finally, being a nondestructive method, microCT can be used *in situ*, thus allowing time-course experiments on the same sample.

VI. CONCLUSION

X-ray microCT was used for the first time to characterize the microstructure of biological and inorganic fouling on a membrane-less SCMFC cathode exposed to primary wastewater for six months. SEM–EDX confirmed the presence of a carbonate layer, with Na^+ and Ca^{2+} as the predominant cations on the outer and inner side of the cathode, respectively. The 3D reconstruction of the fouling on the inner side of the cathode shows that a thin, patchy biofilm grew above a thick, geometrical complex but uninterrupted layer of calcium carbonate and that the latter penetrates the electrode in correspondence to macroscopic surface defects.

The formation of that thick inorganic fouling might influence negatively the cathode performance during long-term operation. These results confirm that microCT is a promising methodology for morphological characterization and mapping of bioelectrochemical systems.

ACKNOWLEDGMENTS

Research fund grant to M. Santini "Progetto ITALY®—Azione 3" and even the prize "5 per 1000" of the University of Bergamo (Italy) are gratefully acknowledged. S. Fest-Santini acknowledges funding by Pro Universitate Bergomensi within their internationalization project. The authors would like also to gratefully acknowledge the Electrochemical Society and Bill & Melinda Gates Foundation under initiative: "Applying Electrochemistry to Complex Global Challenges."

[1]U. Schröder, Phys. Chem. Chem. Phys. **9**, 2619 (2007).
[2]M. Y. El-Naggar, G. Wanger, K. M. Leung, T. D. Yuzvinsky, G. Southam, J. Yang, W. M. Lau, K. H. Nealson, and Y. A. Gorby, Proc. Natl. Acad. Sci. U. S. A. **107**, 18127 (2010).
[3]K. Rabaey, J. Rodrıguez, L. L. Blackall, J. Keller, P. Gross, D. Batstone, W. Verstraete, and K. H. Nealson, ISME J. **1**, 9 (2007).
[4]J. Wei, P. Liang, and X. Huang, Bioresour. Technol. **102**, 9335 (2011). C.
[5]Santoro, M. Guilizzoni, J. P. Correa Baena, U. Pasaogullari, A. Casalegno, B. Li, S. Babanova, K. Artyushkova, and P. Atanassov, Carbon **67**, 128 (2014).
[6]A. Dewan, H. Beyenal, and Z. Lewandowski, Environ. Sci. Technol. **42**, 7643 (2008).
[7]H. Rismani-Yazdia, S. M. Carver, A. D. Christy, and O. H. Tuovinen, J. Power Sources **180**, 683 (2008).
[8]E. Antolini, Biosens. Bioelectron. **69**, 54 (2015).
[9]C. Santoro, A. Serov, C. W. Narvaez Villarrubia, S. Stariha, S. Babanova, A. J. Schuler, K. Artyushkova, and P. Atanassov, ChemSusChem **8**, 828 (2015).
[10]Z. Wang, C. Cao, Y. Zheng, S. Chen, and F. Zhao, ChemElectroChem **1**, 1813 (2014).
[11]C. Santoro, S. Babanova, P. Atanassov, B. Li, I. Ieropoulos, and P. Cristiani, J. Electrochem. Soc. **160**, H720 (2013).
[12]O. Schaetzle, F. Barriere, and U. Schröder, Energy Environ. Sci. **2**, 96 (2009).
[13]J. K. Jang, J. Kan, O. Bretschger, Y. A. Gorby, L. Hsu, B. Kim, and K. H. Nealson, J. Microbiol. Biotechnol. **23**, 1765 (2013).
[14]M. Rimboud, E. Desmond-Le Quemener, B. Erable, T. Bouchez, and A. Bergel, Bioelectrochemistry **102**, 42 (2015).

[15]A. Rinaldi, B. Mecheri, V. Garavaglia, S. Licoccia, P. Di Nardo, and E. Traversa, Energy Environ. Sci. **1**, 417 (2008).
[16]P. Cristiani, A. Franzetti, I. Gandolfi, E. Guerrini, and G. Bestetti, Int. Biodeterior Biodegrad. **84**, 211 (2013).
[17]P. Cristiani, M. L. Carvalho, E. Guerrini, M. Daghio, C. Santoro, and B. Li, Bioelectrochemistry **92**, 6 (2013).
[18]S. Ishii, S. Suzuki, T. M. Norden-Krichmar, T. Phan, G. Wanger, K. H. Nealson, Y. Sekiguchi, Y. A. Gorby, and O. Bretschger, ISME J. **8**, 963 (2014).
[19]S. Ishii, S. Suzuki, T. M. Norden-Krichmar, A. Wu, Y. Yamanaka, K. H. Nealson, and O. Bretschger, Water Res. **47**, 7120 (2013).
[20]W. G. Characklis and K. C. Marshall, *Biofilms* (Wiley, New York, 1990).
[21]H. C. Flemming and J. Wingender, Nat. Rev. Microbiol. **8**, 623 (2010).
[22]*Microbial Extracellular Polymeric Substances: Characterization, Structure and Function*, edited by J. Wingender, T. R. Neu, and H. C. Flemming (Springer-Verlag, New York, 1999).
[23]J. R. Lawrence, D. R. Korber, B. D. Hoyle, J. W. Costerton, and D. E. Caldwell, J. Bacteriol. **173**, 6558 (1991).
[24]J. Schmitt and H. C. Flemming, Int. Biodeterior. Biodegrad. **41**, 1 (1998).
[25]V. Lazarova and J. Manem, Water Res. **29**, 2227 (1995).
[26]S. B. Surman *et al*., J. Microbiol. Method **25**, 57 (1996).
[27]I. B. Beech and R. Tapper, "Microscopy methods for studying biofilms," in *Biofilms: Recent Advances in their Study and Control*, edited by L. S. Evans (Harwood Academic, Amsterdam, 2000), pp. 51–70.
[28]H. Resat, R. S. Renslow, and H. Beyenal, Biofouling **30**, 1141 (2014).
[29]H. Beyenal, C. C. Davis, and Z. Lewandowski, J. Microbiol. Method **58**, 367 (2004).
[30]E. Guerrini, M. Grattieri, S. P. Trasatti, and P. Cristiani, Int. J. Hydrogen Energy **39**, 21837 (2014).
[31]Y. Yuan, S. Zhou, and J. Tang, Environ. Sci. Technol. **47**, 4911 (2013). J.
[32]T. Babauta, H. D. Nguyen, O. Istanbullu, and H. Beyenal, ChemSusChem **6**, 1252 (2013).
[33]M. Grattieri, S. Babanova, C. Santoro, E. Guerrini, S. P. M. Trasatti, P. Cristiani, M. Bestetti, and P. Atanassov, Electroanalysis **27**, 327 (2015). X.
[34]Yang, H. Beyenal, G. Harkin, and Z. Lewandowski, J. Microbiol. Method **39**, 109 (2000).
[35]H. Beyenal, Z. Lewandowski, and G. Harkin, Biofouling **20**, 1 (2004).
[36]C. Santoro, Y. Lei, B. Li, and P. Cristiani, Biochem. Eng. J. **62**, 8 (2012). E.
[37]Guerrini, M. Grattieri, A. Faggianelli, P. Cristiani, and S. Trasatti, Bioelectrochem. **106**, 240 (2015).
[38]M. Santini, M. Guilizzoni, S. Fest-Santini, and M. Lorenzi, Rev. Sci. Instrum. **86**, 023708 (2015).
[39]M. Santini, M. Guilizzoni, and S. Fest-Santini, J. Colloid Interface Sci. **409**, 204 (2013).
[40]M. Santini and M. Guilizzoni, Colloids Interface Sci. Commun. **1**, 14 (2014).
[41]M. Guilizzoni, M. Santini, M. Lorenzi, V. Knisel, and S. Fest-Santini, J. Phys.: Conf. Ser. **547**, 012028 (2014).
[42]L. A. Feldkamp, L. C. Davis, and J. W. Kress, J. Opt. Soc. Am. A **1**, 612 (1984).
[43]D. Jiang, M. Curtis, E. Troop, K. Scheible, J. McGrath, B. Hu, S. Suib, D. Raymond, and B. Li, Int. J. Hydrogen Energy **36**, 876 (2011).
[44]F. Zhang, D. Pant, and B. E. Logan, Biosens. Bioelectron. **30**, 49 (2011). X.
[45]Zhang, D. Pant, F. Zhang, J. Liu, W. He, and B. E. Logan, ChemElectroChem **1**, 1859 (2014).
[46]C. Santoro, A. Stadlhofer, V. Hacker, G. Squadrito, U. Schröder, and B. Li. J. Power Sources **243**, 499 (2013).
[47]C. Santoro, M. Cremins, U. Pasaogullari, M. Guilizzoni, A. Casalegno, A. Mackay, and B. Li, J. Electrochem. Soc. **160**, G3128 (2013).
[48]C. Santoro, I. Ieropoulos, J. Greenman, P. Cristiani, T. Vadas, A. Mackay, and B. Li, J. Power Sources **238**, 190 (2013).
[49]J. Benzinger, J. Nehlsen, D. Blackwell, T. Brennan, and J. Itescu, J. Membr. Sci. **261**, 98 (2005).
[50]S. Babanova, K. Artyushkova, Y. Ulyanova, S. Singhal, and P. Atanassov, J. Power Sources **245**, 389 (2014).
[51]K. Kinoshita, *Electrochemical Oxygen Technology* (Wiley, New York, 1992).
[52]B. Erable, D. Feron, and A. Bergel, ChemSusChem **5**, 975 (2012).
[53]E. Guerrini, P. Cristiani, and S. P. Trasatti, Int. J. Hydrogen Energy **38**, 345 (2013).
[54]S. C. Popat, D. Ki, B. E. Rittmann, and C. I. Torres, ChemSusChem **5**, 1071 (2012).
[55]J. C. Biffinger, J. Pietron, R. Ray, B. Little, and B. R. Ringeisen, Biosens. Bioelectron. **22**, 1672 (2007).